Examination of level density prescriptions for the interpretation of high-energy γ-ray spectra

Srijit Bhattacharya,[1] Deepak Pandit,[2] Balaram Dey,[2] Debasish Mondal,[2] S. Mukhopadhyay,[2] Surajit Pal,[2] A. De,[3] and S. R. Banerjee[2,*]

[1]*Department of Physics, Barasat Government College, Barasat, N 24 Pgs, Kolkata-700124, India*
[2]*Variable Energy Cyclotron Centre, 1/AF, Bidhannagar, Kolkata-700064, India*
[3]*Department of Physics, Raniganj Girls' College, Raniganj-713358, India*

(Received 9 June 2014; revised manuscript received 22 September 2014; published 17 November 2014)

High-energy γ-ray spectra measured by our group involving the compound nuclei (CN) ^{63}Cu at excitation energy $E^* \sim 36$ MeV with average angular momentum $J = 12$–$17\,\hbar$, ^{97}Tc at $E^* \sim 29$–50 MeV with $J = 12$–$14\,\hbar$, ^{113}Sb at $E^* = 109$ and 121 MeV with $J = 49$–$59\,\hbar$, and ^{201}Tl at $E^* = 39.5$ and 47.5 MeV with $J = 18$–$24\,\hbar$ have been analyzed utilizing the level density prescriptions of (i) Ignatyuk, Smirenkin, and Tishin (IST), (ii) Budtz-Jorgensen and Knitter (BJK), and (iii) Kataria, Ramamurthy, and Kapoor (KRK). These three prescriptions have been tested for the correct statistical model description of high-energy γ rays in the light of extracting the giant dipole resonance (GDR) parameters at low excitation energy and spin where shell effects might play an important role, as well as at high excitation energy where shell effects have melted. Interestingly, only the IST level density prescription could explain the high-energy γ-ray spectra with reasonable GDR parameters for all four nuclei.

DOI: 10.1103/PhysRevC.90.054319 PACS number(s): 21.10.Ma, 24.30.Cz, 24.60.Dr, 25.70.Gh

I. INTRODUCTION

One of the most exciting topics in contemporary nuclear physics is the study of nuclear structure under extreme conditions of nuclear temperature T and angular momentum J. The giant dipole resonance (GDR), an archetypical example of collective vibrational mode built on excited nuclear states, provides us insight into exotic nuclear shapes and structures [1–3]. Ardent experimental and theoretical interests [4–22] can be seen over the years in studying the properties of the GDR built on excited states in nuclei as this collective mode is strongly coupled to nuclear damping and shape degrees of freedom. The strength $S_{\rm GDR}$, centroid energy $E_{\rm GDR}$, and width $\Gamma_{\rm GDR}$ are the parameters that describe a GDR strength function. The knowledge in $E_{\rm GDR}$ provides better understanding of the symmetry energy of nuclear matter while the systematic study of $\Gamma_{\rm GDR}$ with T sheds light on the characteristics of damping prevailing within the nuclear matter as well as the evolution of deformations embodied within it [23].

Measurement of high-energy γ rays ($E_\gamma = 8$–20 MeV) from the decay of hot compound nucleus (CN) is one of the most important probes for studying the GDR in excited nuclei. To understand the properties of the GDR parameters in excited nuclei, the characterization of the measured high-energy γ rays and its comparison with the predictions of theoretical statistical model related to CN decay are absolutely necessary. However, the acceptability of any statistical model prediction depends on its essential ingredient, the nuclear level density, which is also the central source of uncertainty in analyzing nuclear reactions and in the reliable extraction of the GDR quantities, i.e., $S_{\rm GDR}$, $E_{\rm GDR}$, and $\Gamma_{\rm GDR}$.

It is an important fact that the level density of excited nuclei is strongly influenced by the nuclear shell structure that melts down with the increase in excitation energy E^* of the nucleus. Although for high spin and high E^* the shell structure might not be melted near the yrast line. The reliable extraction of the GDR Lorentzian not only depends on the statistical model predictions for the region $E_\gamma = 8$–20 MeV of the high-energy γ-ray spectrum but also on the statistical part ($E_\gamma \leqslant 8$ MeV) of the spectrum. The statistical part is highly sensitive to the level density of the decaying nuclei, especially in the later part of the decay chain where the shell effect is extremely important. Angular momentum J as well as the evolution of nuclear deformation in the CN decay chain also play leading roles in the modification of nuclear level density. Therefore, the statistical model must include a proper level density formalism as input, which can take care of all these facts.

The basic nuclear level density formula, derived from the back-shifted Fermi gas model and based on the pioneering work of Bethe [24], is given by

$$\rho(E^*, J) = \frac{2J+1}{12I^{3/2}}\sqrt{a}\frac{\exp\left[2\sqrt{(aU)}\right]}{U^2}, \tag{1}$$

where $U = E^* - \Delta - J(J+1)\hbar^2/2I$ is the available thermal energy. The effective moment of inertia of the compound nucleus is taken as $I = I_0(1 + \delta_1 J^2 + \delta_2 J^4)$, where I_0 is the spherical rigid body moment of inertia while δ_1 and δ_2 are the deformability coefficients. The excitation energy is back-shifted by the pairing energy $\Delta = 12/\sqrt{A}$, A being the mass number of the nucleus. a is the level density parameter and is taken as an adjustable free parameter.

In the Fermi gas model the level density depends on the level density parameter a which, in turn, is related to the finite size effect of the nuclear matter, the effective mass of the nucleon, and the number of single-particle levels near the Fermi surface. All of these depend on nuclear deformation, shell structure of the nucleus, and also how the shell structure gradually

*srb@vecc.gov.in

melts with the increase in E^* of the nucleus. Pühlhofer's [25] statistical model code CASCADE includes formulation of level density parameter a as per Dilg [26] for $E^* < 10$ MeV. For $E^* > 20$ MeV, $a = A/k$ was used, based on the liquid drop model, where k is user-dependent free inverse level density parameter and A is the nuclear mass. For E^* ranging from 10–20 MeV, linear interpolation of a and Δ is done midway between the parametrization of Dilg and that of the liquid drop model. But the noninclusion of the proper treatment of the shell corrections and its washing out at higher excitation energies along with the effect of nuclear deformation induces large uncertainty [5] in explaining the high-energy γ-ray spectra when the Dilg formulation is used.

An ideal level density prescription should describe level density correctly starting from lower to higher E^* at different J values. It should also incorporate shell effects at lower E^* smoothly connecting to the liquid drop behavior of the nucleus at higher E^* and it must describe the high-energy γ-ray spectra faithfully. The existing level density formulation by Ignatyuk, Smirenkin, and Tishin (IST) [27] is quite popular as it can predict high-energy γ rays at different excitations. Besides IST, a few other modified theoretical as well as empirical level density prescriptions also exist in the literature. Two such level density prescriptions are of Kataria, Ramamurthy, and Kapoor (KRK) [28], and Budtz-Jorgensen and Knitter (BJK) [29]. Dioszegi *et al.* [30] have shown a comparative study between Dilg, IST, and BJK level density formalisms for $A = 110$–130 over the excitation energy range 58–62 MeV ($T = 1.98$–2.23 MeV) and angular momentum 16.9–20.9 $\hbar$ by matching experimental high-energy γ-ray spectra with CASCADE predictions. They pointed toward the superiority of IST level density over the others (Dilg and BJK) in the said E^* region and also could not find any change of the GDR parameters even after including different level density prescriptions within the statistical model. However, they did not test the IST level density prescription at lower temperatures where the shell structure is important. Moreover, the other two prescriptions (KRK and BJK) have never been used in describing the high-energy γ-ray spectra for different nuclei at different excitation energies.

In this work, the KRK, BJK, and IST level density formalisms are rigorously tested at lower excitation energy ranges $E^* \sim 29$–50 MeV and lower spin (12–17 $\hbar$) for the CN ^{97}Tc and ^{63}Cu as well as at higher excitation energy $E^* \sim 109$–121 MeV and higher spin (49–59 $\hbar$) for ^{113}Sb. In addition, the applicability of IST and KRK level density prescriptions are investigated on the high-energy γ-ray spectra of ^{201}Tl, in which the ground-state shell correction energy is larger than those of ^{63}Cu, ^{97}Tc, and ^{113}Sb. Here, the advantage of populating these nonfissioning nuclei, having a spherical ground state, is that the user-dependent free parameters in CASCADE decrease considerably and a one-component GDR strength function can be extracted reliably. As a result, it becomes much easier to test the CASCADE predictions giving full emphasis only on the level density input. Moreover, we chose the KRK level density rather than that of Dilg *et al.* because the former incorporates the shell structure of nuclei at lower E^* and also its extrapolation to higher energies.

II. EXPERIMENTAL DETAILS

Very recently, a large amount of experimental data [12,15,17,19] on high-energy γ-ray ($E_\gamma = 4$–32 MeV) measurements have been reported in different nuclei and in varying excitation energies as well as angular momenta for studying the properties of the GDR modes in nuclei. Using the α beam from the K-130 cyclotron at the Variable Energy Cyclotron Centre, Kolkata, a self-supporting 1 mg/cm^2 thick ^{93}Nb target was bombarded at the projectile energies of 28, 35, 42, and 50 MeV populating the compound nucleus ^{97}Tc at the excitation energies of 29.3, 36, 43, and 50.4 MeV, respectively [19]. The compound nuclei were populated in the angular momentum window 12–21 $\hbar$. The high-energy γ spectra were measured by means of a part (49 detectors in the form 7×7 matrix) of the LAMBDA array [31]. The array was placed at a distance of 50 cm from the target and at an angle of 90° with the beam axis. The angular momentum populated by the compound nucleus was measured with a 50-element low-energy γ-multiplicity detector array [32]. To measure the inverse level density parameter k at different energies, the evaporated neutron energy spectra were extracted by converting the time-of-flight data of BC501A liquid scintillators [33]. In other nuclear reactions ^{4}He + ^{59}Co, ^{20}Ne + ^{93}Nb, and ^{4}He + ^{197}Au, the compound nuclei ^{63}Cu, ^{113}Sb, and ^{201}Tl were populated for the beam energies of $E_{\rm lab} = 35$ MeV, 145 and 160 MeV, and 42 and 50 MeV, respectively. The details of the experiments are explained elsewhere [12,17].

III. ADOPTED LEVEL DENSITIES

The experimental spectra of high-energy γ rays coming from the decay of the compound nuclei (^{63}Cu, ^{97}Tc, ^{113}Sb, and ^{201}Tl) were fitted with the CASCADE predictions, using different level density prescriptions, folded with the detector response along with an exponential bremsstrahlung component given by $\exp(-E_\gamma/E_0)$ (E_0 is the slope parameter). The bremsstrahlung slope parameter E_0 was obtained from the systematics $E_0 = 1.1[(E_{\rm lab} - V_c)/A_p]^{0.72}$, where $E_{\rm lab}$, V_c, and A_p represent the beam energy, Coulomb barrier, and projectile mass, respectively [34]. Corresponding experimental angular momentum distribution, $E_{\rm GDR}$, $S_{\rm GDR}$, and $\Gamma_{\rm GDR}$ were taken as CASCADE inputs. The GDR parameters were extracted by the χ^2 best fit CASCADE predictions (in the range $E_\gamma = 10$–20 MeV). For all the three level density prescriptions, at a common beam energy, the bremsstrahlung slope parameter E_0 was kept fixed as per systematics and only the GDR strengths, widths, and centroid energies were varied.

A. KRK level density prescription

The semiempirical model proposed by KRK [28] on nuclear level density is important for the statistical modeling of nuclear decay because it incorporates the shell effects and their E^* dependence. The excitation energy and spin-dependent level density $\rho(E^*, J)$, related with state density $W(E^*)$, adopted

in this model are given by

$$\rho(E^*,J) = \frac{(2J+1)W(E^*)}{2\sqrt{(2\pi)}\sigma^3(E^*)} \exp\frac{-J(J+1)}{2\sigma^2(E^*)}, \quad (2)$$

$$W(E^*) = C\exp S(E^*), \quad (3)$$

where σ is the spin cutoff parameter that depends on the effective moment of inertia of the nucleus. The state density $W(E^*)$ is related to the entropy S, a function of excitation energy. E^* and the temperature T of the excited nucleus are interconnected by the level density parameter a. Unlike other level density formalisms, KRK proposes the level density parameter as shell independent, similar to that of a nucleus under the liquid drop model. Here, the shell structure influences the level density with a ground-state shell correction energy term added in the total nuclear E^*.

In KRK model, the analytical expressions of entropy and excitation energy can be achieved after detailed calculation as

$$S = \frac{1}{3}\pi^2 g_0 T + \frac{A_1}{T}\frac{\pi^2\omega^2\cosh(\pi\omega T)}{\sinh^2(\pi\omega T)} - \frac{\pi\omega T}{\sinh\pi\omega T}, \quad (4)$$

$$E^* = \frac{1}{6}\pi^2 g_0 T^2 + A_1\frac{\pi^2\omega^2 T^2\cosh(\pi\omega T)}{\sinh^2(\pi\omega T)}, \quad (5)$$

where A_1, the ground-state shell correction energy, depends on the fundamental frequency of oscillation of the fluctuating part in the level density (ω). At large temperature limit, one gets $S = \pi^2 g_0 T/3$ and $E^* = -A_1 + \pi^2 g_0 T^2/6$, where g_0 is the density of single-particle states proportional to the level density parameter a. These equations may be used as the framework to calculate the level density parameter as a function of E^* with known values of ground-state shell correction energies. The constants α, β, and ω_0 can be estimated by comparing the theoretical nuclear level spacing with the experimental level spacing obtained from the neutron resonance data at $E^* \sim 10$ MeV. These constants are related to the level density parameter and the frequency of shell oscillation (ω) by $a = \alpha A(1-\beta A^{-1/3}B_s)$ and $\omega = \omega_0 A^{-1/3}$, where B_s is the surface area relative to that of a sphere of the same volume. The reported best fit values were [28] $\alpha = 0.18$ MeV^{-1}, $\beta = 1.0$, and $\omega_0 = 0.185$ MeV^{-1}.

KRK found that the level density calculated with their model successfully agrees with the experimental data up to the excitation energy around 25 MeV for the nuclei ^{56}Fe and ^{55}Mn [35]. The mass-dependent level density parameters calculated by KRK for spherical nuclei are shown in Fig. 1. Unfortunately, the KRK model has not been used in the past for the extraction of GDR parameters.

B. BJK level density prescription

The second of the three nuclear level density prescriptions used in this work is that of BJK. The experimentally measured and compiled values of mass-dependent level density parameters obtained by BJK [29] for the nuclei ranging from $90 \leqslant A \leqslant 165$ are shown in Fig. 1. These level density parameters were extracted from neutron evaporation measurements in the spontaneous fission of ^{252}Cf.

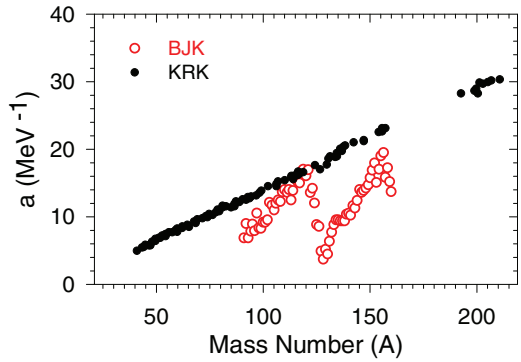

FIG. 1. (Color online) Mass-dependent level density parameters calculated by Kataria (i.e., KRK) for spherical nuclei and the level density parameters compiled by BJK from the experimental data on the spontaneous fission of ^{252}Cf.

C. IST level density prescription

The model proposed by IST [27] involves the improved E^*-dependent level density parameter a. In this model the level density parameter is given by

$$a(U) = \tilde{a}\left(1 + \frac{\delta W}{U}(1-\exp(-\gamma U))\right). \quad (6)$$

This parametrization incorporates the effect of nuclear shell structure at lower excitation energy and extrapolates to the smooth liquid drop behavior at higher excitation energy where the shell effect is expected to be melted. δW is the shell correction factor, which is the difference between the experimental and the liquid drop masses. γ^{-1} is the rate at which shell effects melt as E^* increases and it is generally taken as 18.5 MeV. $\tilde{a}$ is the asymptotic Fermi gas level density parameter and is taken as a user-dependent free parameter. In partial modification of this formula, Reisdorf [36] showed that the asymptotic level density parameter depends on the mass of the compound nucleus as well as the nuclear deformation, given by

$$\tilde{a} = 0.04543 r_0^3 + 0.1355 r_0^2 A^{-1/3} B_s + 0.1426 r_0 A^{-2/3} B_k, \quad (7)$$

where B_s and B_k are the nuclear surface and curvature terms, respectively, and taken as unity for spherical nuclei. r_0, the nuclear radius parameter, is taken as 1.15 fm.

IV. RESULTS AND DISCUSSION

In view of the available high-energy γ-ray spectra measured by our group for the compound nuclei ^{63}Cu, ^{97}Tc, ^{113}Sb, and ^{201}Tl over a wide range of excitation energies 29.3–109 MeV and angular momenta 12–59 $\hbar$, we attempt here to assess the applicability of the three level density prescriptions. ^{63}Cu, ^{97}Tc, and ^{113}Sb all have lower ground-state shell correction energies (1.86, 1.26, and 1.54 MeV, respectively). On the other hand, ^{201}Tl has a higher ground-state shell correction energy of -8.27 MeV. While the other three nuclei were all populated at lower E^* and J, ^{113}Sb was populated at higher E^* and J values.

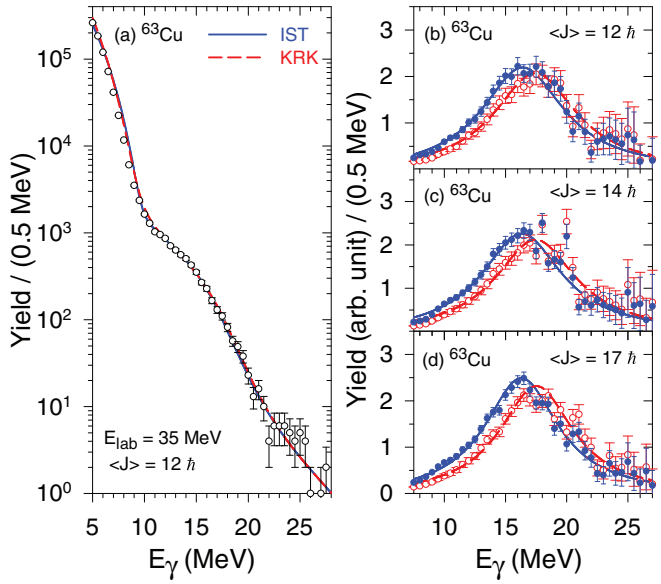

FIG. 2. (Color online) (a) Experimental high-energy γ-ray spectra (open circles with error bars) for the reaction ^{4}He + ^{59}Co at projectile energy 35 MeV along with the CASCADE predictions utilizing KRK (red dashed line) and IST (blue continuous line) level density formalisms. (b)–(d) Corresponding experimental linearized divided plots at different angular momenta with IST (filled circles with blue continuous line) and KRK (open circles with red dashed line) level density prescriptions.

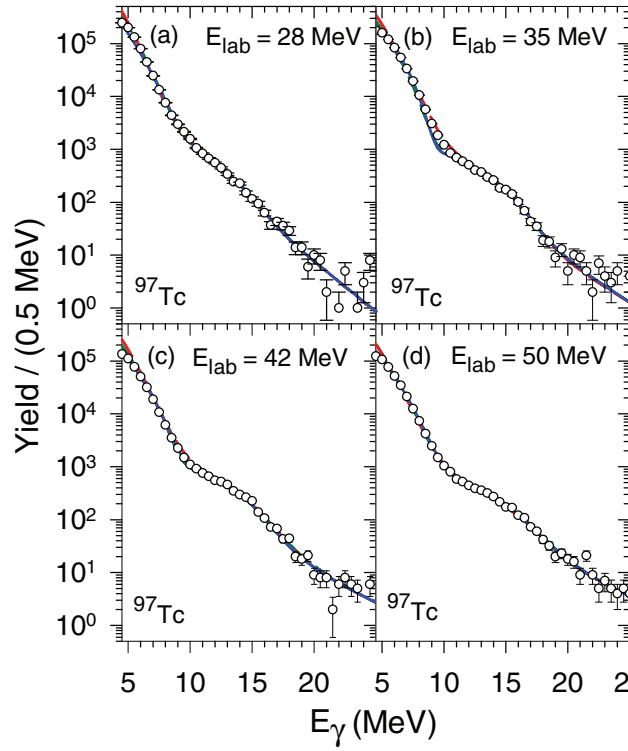

FIG. 3. (Color online) Experimental high-energy γ-ray spectra (open circles with error bars) for the reaction ^{4}He + ^{93}Nb at projectile energies 28, 35, 42, and 50 MeV along with CASCADE predictions utilizing KRK (red dashed line), BJK (green dotted-dashed line), and IST (blue continuous line) level density formalisms.

A. ^{63}Cu

The experimental high-energy γ-ray spectrum for the compound nucleus ^{63}Cu at projectile energy 35 MeV ($E^* =$ 36 MeV) and CN average angular momentum $J = 12$ $\hbar$ is shown in Fig. 2(a) by open circles. The CASCADE predictions utilizing IST and KRK level density prescriptions are also included in the same figure. It is highly interesting to note that both the IST and KRK level density formalisms included in CASCADE represent the high-energy γ-ray spectra equally well. However, the extracted GDR centroid energies are very different. The discrepancy is evident in the linearized GDR plots shown in Figs. 2(b)–2(d) for J=12, 14, and 17 $\hbar$ using the quantity $F(E_\gamma)Y^{\rm expt}(E_\gamma)/Y^{\rm cal}(E_\gamma)$, where, $Y^{\rm expt}(E_\gamma)$ and $Y^{\rm cal}(E_\gamma)$ are the experimental and the best fit CASCADE spectra, corresponding to a single Lorentzian function $F(E_\gamma)$. The GDR centroid energy extracted at different J using the KRK prescription comes out to be 17.9 MeV. This value is slightly larger than the existing systematics of GDR built on the excited state: $E_{\rm GDR} = 18A^{-1/3} + 25A^{-1/6}$ [1], which predicts 17.0 MeV.

In contrast, the IST level density included in CASCADE successfully predicts the high-energy γ-ray spectra for ^{63}Cu with $E_{\rm GDR}$ coming out between 16.7 and 16.9 MeV, much closer to the systematics. Unfortunately, it was not possible to test the BJK level density for the nucleus ^{63}Cu because the lower mass $A = 63$ does not fall under the mass distribution of the ^{252}Cf fission fragments.

B. ^{97}Tc

The experimental high-energy γ-ray spectra for ^{97}Tc at projectile energies of 28, 35, 42, and 50 MeV corresponding to $E^* = 29.3$, 36.0, 43.0, and 50.4 MeV are shown in Figs. 3(a)–3(d) along with CASCADE predictions utilizing KRK (red dashed lines), BJK (green dotted-dashed line), and IST (blue continuous line) level density prescriptions. For better understanding of the GDR strength function, the corresponding linearized divided plots are shown in Fig. 4. The comparison of IST and KRK prescriptions is demonstrated in the Figs. 4(a)–4(d), while a similar comparison of IST and BJK prescriptions is shown in Figs. 4(e)–4(h). The corresponding CN average J values are also quoted in all the figures.

Here the linearized GDR Lorentzians once again corroborate the similar trend observed in ^{63}Cu. The KRK prescription explains the GDR line shape well but with higher values of $E_{\rm GDR}$.The extracted best fit $E_{\rm GDR}$ is found to be lying between 17.0-17.5 MeV, much higher than the value of 15.6 MeV as per the existing systematics, except for $E_{\rm lab} = 28$ MeV in which the best fit value comes out to be 15.8 MeV closer to the systematics. It is worthwhile to mention that not only the CN ^{97}Tc is populated in lower excitation energy ranges but also the compound nuclear angular momentum lies in lower side between 12 to 14 $\hbar$.

The statistical model code CASCADE using the BJK prescription can predict high-energy γ-ray spectra reasonably well for ^{97}Tc at all excitation energies. However, in contrast

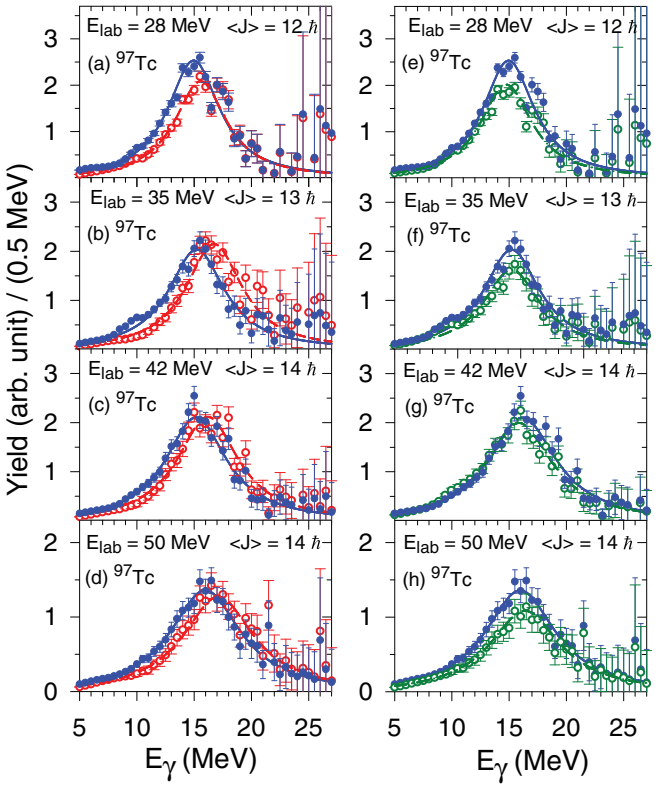

FIG. 4. (Color online) Experimental linearized plots for the reaction ^{4}He + ^{93}Nb at projectile energies 28, 35, 42, and 50 MeV along with CASCADE predictions utilizing KRK (open circles with red dashed line) and IST (filled circles blue continuous line) level density formalisms in (a)–(d) and BJK (open circles with green dotted-dashed line) and IST (filled circles with blue continuous line) in (e)–(h).

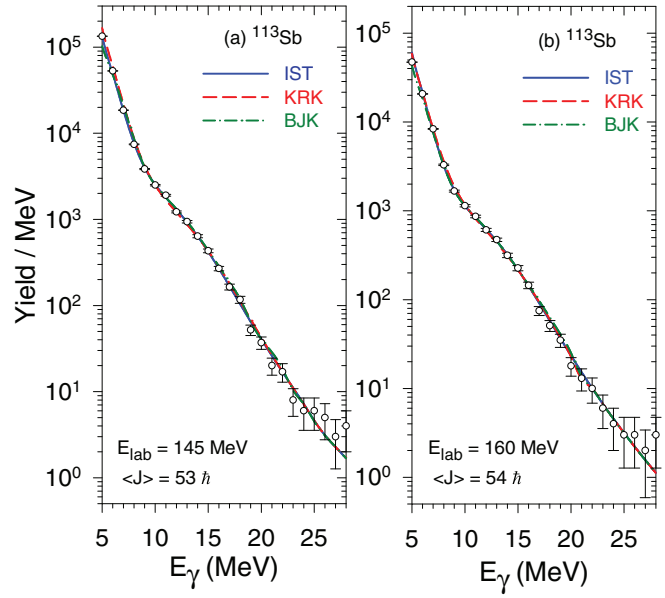

FIG. 5. (Color online) Experimental high-energy γ-ray spectrum (open circles with error bars) for the reaction ^{20}Ne + ^{93}Nb along with CASCADE predictions exploiting KRK, BJK, and IST level density formalisms at projectile energies of (a) 145 and (b) 160 MeV.

to KRK, the best fit GDR centroid energies vary between 15.0 and 16.8 MeV.

All the experimental data for the decay of the CN ^{97}Tc are found to be in good agreement with the CASCADE prediction utilizing the IST level density prescription. The extracted best fit $E_{\rm GDR}$ remains close to the value 15.6 MeV in agreement with the GDR systematics, except for $E_{\rm lab}$ = 50 MeV in which the estimated GDR peak energy is around 16.4 MeV. In all these data sets, the user-dependent input $\tilde{a}$ is taken as $A/8.0$, $A/9.7$, $A/9.0$, and $A/9.2$ MeV^{-1} at $E_{\rm lab}$ = 28, 35, 42, and 50 MeV, respectively, as extracted from the neutron evaporation data [19].

C. ^{113}Sb

To understand the effect of level density prescriptions at higher angular momentum and higher excitation energy domains, the three level density prescriptions were used to explain the experimental data of high-energy γ rays measured for the compound nucleus ^{113}Sb [12]. The experimental data along with KRK, BJK, and IST predictions are shown in Fig. 5 for $E_{\rm lab}$ = 145 MeV (E^* = 109 MeV) and average J = 53 $\hbar$ and for $E_{\rm lab}$ = 160 MeV (E^* = 121 MeV) and average J = 54 $\hbar$. The difference between KRK and IST predictions can be well understood through linearized plots shown in Figs. 6(a)–6(e) at $E_{\rm lab}$ = 145 and 160 MeV for different average CN angular momenta. Similarly, Figs. 6(f)–6(j) interpret the difference between IST and BJK predictions at similar projectile energies and average J. At higher J values (49–59 $\hbar$), for the IST prescription, the asymptotic level density parameter was not measured and therefore $\tilde{a}$ is chosen as $A/8.0$ MeV^{-1} according to the Reisdorf formula [36]. The change in $\tilde{a}$ from $A/8.0$ to $A/9.0$ MeV $^{-1}$ could only alter the extracted $E_{\rm GDR}$ and $S_{\rm GDR}$ by 3% and 5%, respectively. For ^{113}Sb, the IST prescription explains the experimental data very well and $E_{\rm GDR}$ = 15.5 MeV comes out to be consistent with the prediction (15.1 MeV) of the existing systematics. However, the KRK prescription can explain the data only if $E_{\rm GDR}$ is taken as 17.0–17.3 MeV, much larger than the existing systematics. The BJK prescription can also explain the data but with much lower values of $E_{\rm GDR}$ (14.0 MeV).

D. ^{201}Tl

The suitability of each of the three level density prescriptions was also investigated in higher nuclear mass regions using another set of experimental data [17] for the reaction ^{4}He + ^{197}Au at $E_{\rm lab}$ = 50 MeV (E^* = 47.5 MeV) and $E_{\rm lab}$ = 42 MeV (E^* = 39.5 MeV) at lower compound nuclear J values (18–24 $\hbar$). The experimental high-energy γ spectra are shown along with IST and KRK prescriptions in Figs. 7(a) and 8(a). The corresponding linearized plots are shown in Figs. 7(b), 7(c), 8(b), and 8(c). Again a similar trend has been found in which the KRK-predicted best fit $E_{\rm GDR}$ comes out to be larger (14.4–14.7 MeV) than the excited-state GDR centroid energy systematics (13.4 MeV), while the IST predictions of $E_{\rm GDR}$ (13.5–13.9 MeV) remain in agreement with the systematics. In the IST prescription, $\tilde{a}$ was taken as $A/8.0$ MeV^{-1}. It was

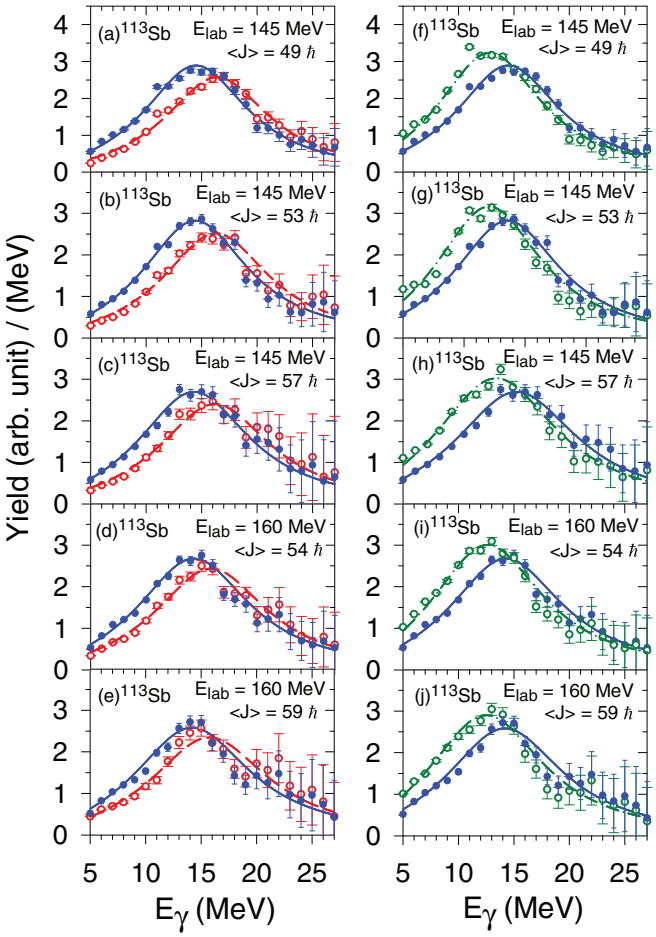

FIG. 6. (Color online) (a)–(e) Experimental linearized plots for the reaction ^{20}Ne + ^{93}Nb at projectile energies 145 and 160 MeV along with CASCADE predictions utilizing KRK (open circles with red dashed line) and IST (filled circles with blue continuous line) level density formalisms. (f)–(j) Same as above but utilizing BJK (open circles with green dotted-dashed line) and IST (filled circles with blue continuous line) level density formalisms.

not possible to test the BJK level density on the nucleus ^{201}Tl as it does not fall under the mass distribution of ^{252}Cf fission fragment.

E. Discussion

It is highly interesting to note that the high-energy γ-ray spectra for all four nuclei ^{63}Cu, ^{97}Tc, ^{113}Sb, and ^{201}Tl at different excitation energies and angular momenta are described very well using the KRK and IST level density formalism in the CASCADE calculation. The BJK prescription can explain only ^{97}Tc and ^{113}Sb data because the other two nuclei do not fall under the mass distribution of ^{252}Cf fission fragments. However, it is important to mention that the extracted GDR centroid energies come out to be very dissimilar using different level density prescriptions, but the GDR widths remain unchanged in all cases. The extracted values of GDR parameters for the three prescriptions are shown in Table I.

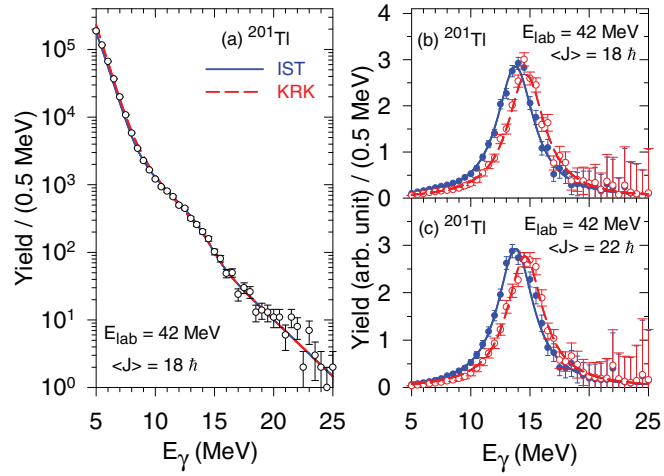

FIG. 7. (Color online) (a) Experimental high-energy γ-ray spectrum (open circles with error bars) for the reaction ^{4}He + ^{197}Au at projectile energy 42 MeV along with the CASCADE predictions using KRK and IST level density formalisms. (b)–(c) Corresponding linearized plots.

Despite testing on varying experimental data with a wide range of E^* and J and ground-state shell correction energies, intriguingly, the KRK prescription consistently predicts higher values of E_{GDR}. The E_{GDR} for the nuclei ^{63}Cu, ^{97}Tc, and ^{113}Sb with smaller ground-state shell correction comes out to be 5, 13, and 12% larger, respectively, than the existing systematics, while for ^{201}Tl with larger ground-state shell correction energy this discrepancy is nearly 10%. It is important to mention here that the KRK formalism is unique in comparison to the other two formalisms, since in this case the shell correction is incorporated through the nuclear excitation energy, instead of modifying the level density parameter. Figures 9(a) and 9(b) show the calculated J-integrated KRK level density as a function of excitation energy E^* along with the IST level density and BJK for the nucleus ^{97}Tc (small shell correction) and ^{201}Tl (large shell correction), respectively. As can be seen,

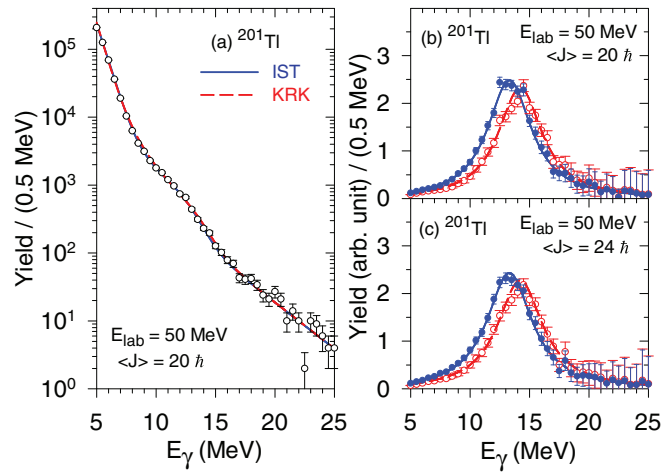

FIG. 8. (Color online) Same as Fig. 7, but for projectile energy 50 MeV.

TABLE I. GDR parameters extracted using different level density prescriptions.

CN	Proj.	E_{lab}	E^*	J_{CN}	E_{GDR} (MeV)			S_{GDR}			Γ_{GDR} (MeV)		
		(MeV)	(MeV)	($\hbar$)	BJK	KRK	IST	BJK	KRK	IST	BJK	KRK	IST
^{63}Cu	^{4}He	35	36.0	12 ± 6		17.9 ± 0.1	16.9 ± 0.1		1.35	1.35		8.2 ± 0.2	8.2 ± 0.2
		35	36.0	14 ± 6		17.9 ± 0.1	16.8 ± 0.1		1.75	1.75		8.0 ± 0.2	8.0 ± 0.2
		35	36.0	17 ± 6		17.9 ± 0.1	16.7 ± 0.1		1.75	1.75		7.3 ± 0.2	7.3 ± 0.2
^{97}Tc	^{4}He	28	29.3	12 ± 6	15.0 ± 0.1	15.8 ± 0.1	15.2 ± 0.1	1.0	1.0	1.20	5.5 ± 0.5	5.5 ± 0.5	5.5 ± 0.5
		35	36.0	13 ± 4	15.5 ± 0.1	17.0 ± 0.1	15.6 ± 0.1	1.1	1.35	1.25	6.0 ± 0.5	6.0 ± 0.5	6.0 ± 0.5
		42	43.0	14 ± 5	15.2 ± 0.1	16.5 ± 0.1	15.5 ± 0.1	1.1	1.30	1.20	6.5 ± 0.5	6.5 ± 0.5	6.5 ± 0.5
		50	50.4	14 ± 5	16.8 ± 0.1	17.5 ± 0.1	16.4 ± 0.1	0.9	1.10	1.10	7.5 ± 0.5	7.5 ± 0.5	7.5 ± 0.5
^{113}Sb	^{20}Ne	145	109.0	49 ± 11	14.0 ± 0.2	17.4 ± 0.2	15.5 ± 0.2	1.0	1.0	1.0	11.6 ± 0.3	11.6 ± 0.3	11.6 ± 0.3
		145	109.0	53 ± 11	14.0 ± 0.2	17.3 ± 0.2	15.5 ± 0.2	1.0	1.0	1.0	11.8 ± 0.3	11.8 ± 0.3	11.8 ± 0.3
		145	109.0	57 ± 11	14.0 ± 0.2	17.3 ± 0.2	15.5 ± 0.2	1.0	1.0	1.0	12.4 ± 0.3	12.4 ± 0.3	12.4 ± 0.3
		160	121.0	54 ± 11	14.0 ± 0.2	17.0 ± 0.2	15.5 ± 0.2	1.0	1.0	1.0	12.5 ± 0.3	12.5 ± 0.3	12.5 ± 0.3
		160	121.0	59 ± 11	14.0 ± 0.2	17.0 ± 0.2	15.5 ± 0.2	1.0	1.0	1.0	13.0 ± 0.3	13.0 ± 0.3	13.0 ± 0.3
^{201}Tl	^{4}He	42	39.5	18 ± 6		14.8 ± 0.3	13.9 ± 0.3		1.0	1.0		3.8 ± 0.5	3.8 ± 0.5
		42	39.5	22 ± 6		14.7 ± 0.3	13.9 ± 0.3		1.0	1.0		3.7 ± 0.5	3.7 ± 0.5
		50	47.5	20 ± 6		14.4 ± 0.3	13.5 ± 0.3		1.0	1.0		4.5 ± 0.5	4.5 ± 0.5
		50	47.5	24 ± 6		14.4 ± 0.3	13.5 ± 0.3		1.0	1.0		4.6 ± 0.5	4.6 ± 0.5

the KRK level density intersects IST at around $E^* = 20$ MeV and thereafter they diverge from each other. This seems to be the possible reason for agreement between KRK and IST predicted data only at the effective E^* (i.e., E^* of 29.3 MeV minus the rotational energy) $\sim$ 20 MeV for ^{97}Tc. In case of higher E^*, the two prescriptions differ. As it appears, the larger GDR centroid energy obtained, in comparison to the systematic, for the KRK prescription could be due to incorrect extrapolation at higher E^* and J.

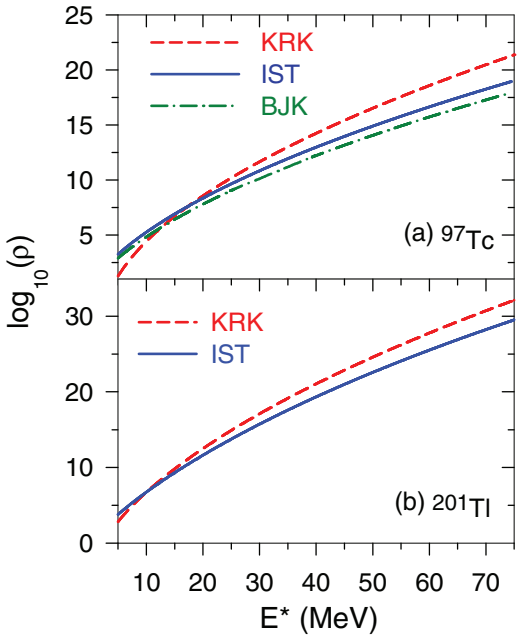

FIG. 9. (Color online) Angular momentum integrated level density as a function of excitation energy E^* for (a) ^{97}Tc using IST, BJK, and KRK prescriptions and (b) ^{201}Tl considering IST and KRK prescriptions.

In Fig. 10 the CASCADE predictions of high-energy γ-ray spectra have been shown utilizing KRK, IST, and BJK level density prescriptions for the nuclei ^{97}Tc at lower E^* and J and for ^{113}Sb at higher E^* and J. The GDR parameters were kept the same for all the three prescriptions. The plots clearly indicate that for the common input parameters the KRK-predicted γ-ray yield at the higher energy side is lower than the with the other two formalisms. This reduced yield is actually compensated for by shifting E_{GDR} at higher energies resulting in higher values of E_{GDR}. It is important to extract the correct centroid energy else it can introduce systematic error in

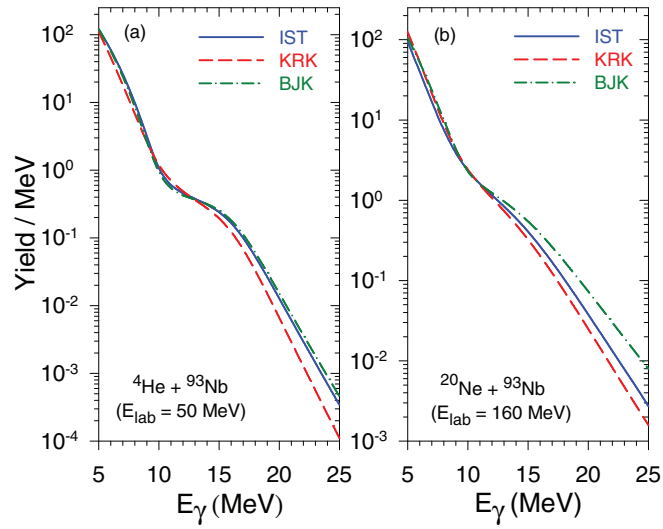

FIG. 10. (Color online) CASCADE outputs of high-energy γ-ray spectrum for (a) the reaction ^{4}He + ^{93}Nb at projectile energy E_{lab} = 50 MeV and (b) the reaction ^{20}Ne + ^{93}Nb at projectile energy E_{lab} = 160 MeV. All the outputs are generated using the same GDR parameters.

the estimation of nuclear temperature for the GDR vibration. Apart from that, a higher value of E_{GDR} would jeopardize the direct comparison between the theoretical and experimental GDR line shapes. Moreover, the proper value of E_{GDR} is also very useful in the exploration of nuclear symmetry energy [23]. Hence, as it appears, the KRK level density prescription may not be used to explain the high-energy γ-ray spectra because it systematically produces higher GDR centroid energy.

It can be fairly inferred that the BJK prediction matches well with the experimental data for different E^* values with reasonable best fit values of the GDR parameters, in so far as the nucleus ^{97}Tc is concerned, which has a very small amount of ground-state deformation as well as lower shell correction energy. However, at higher J and higher E^*, the BJK prescription misinterprets GDR centroid energies for ^{113}Sb (Fig. 9). The inherent problem of the BJK formalism lies in the fact that the compiled level density parameters are independent of E^*. Therefore, for the same mass number, one has to adopt the same set of level density parameters for all values of E^*. This does not have much effect on ^{97}Tc but has an adverse impact on the fitting of experimental spectra of ^{113}Sb. The BJK prediction breaks down not only at higher E^*, but also in the event of high angular momentum. The discrepancy at higher E^* and J is also highlighted in Fig. 10(b). As can be seen, the BJK-predicted γ-ray yield at the higher energy side is much higher than the other two formalisms for the common input GDR parameters. This higher yield is compensated for by shifting E_{GDR} at lower values. Another disadvantage concerned with BJK is that the extracted level density parameters from the neutron decay in ^{252}Cf fission studies can be used reliably only for a system with the same mass and deformation as those available in the BJK compilations. Therefore we could not use the BJK prescription for ^{63}Cu and ^{201}Tl. Moreover, the BJK level density cannot be safely extrapolated to other systems, especially in case of a deformed nucleus as observed earlier [30].

Interestingly, the IST level density formalism quite successfully describes the experimental data for all four nuclei with reasonably correct values of E_{GDR} at all conditions of E^* and J and ground-state shell corrections. Therefore, it can be said that among the three level density prescriptions the IST is the most suitable. The reason being its efficiency to interpret the varying experimental data sets in terms of best fit GDR parameters in agreement with existing systematics.

Recently, several new semiempirical as well as microscopic level density formalisms have also been developed. Nakada and Alhassid calculated level densities [37] under the framework of the Monte Carlo shell model for different nuclei. Von Egidy and Bucurescu [38] also estimated level densities using the Fermi gas model as well as a constant temperature model. It will be interesting in the future to test the applicability of the newer level density formalisms on high-energy γ-ray spectra.

V. CONCLUSION

This work investigates the applicability of three different level density prescriptions viz. KRK, BJK, and IST using experimental high-energy γ-ray spectra for the four nuclei ^{63}Cu, ^{97}Tc, ^{113}Sb, and ^{201}Tl at different excitation energies and angular momenta. The extracted E_{GDR} in the case of the KRK prescription was found to be higher than that of the existing GDR systematics for all four nuclei owing to the prediction of larger values of the nuclear levels at higher excitation energies in comparison to those predicted by the other two formalisms. On the other hand, the BJK prescription predicted lower E_{GDR} compared to systematics in the case of ^{113}Sb at higher E^* and J. Moreover, the BJK could not be tested on ^{63}Cu and ^{201}Tl due to its applicability in a limited mass region. Intriguingly, the IST level density formalism quite successfully described all the data sets both at low and high E^* and J indicating the universality of the IST level density prescription in explaining the high-energy γ-ray spectra with reasonably correct GDR parameters.

[1] J. J. Gaardhoje, Ann. Rev. Nucl. Part. Sci. **42**, 483 (1992).
[2] K. A. Snover, Ann. Rev. Nucl. Part. Sci. **36**, 545 (1986).
[3] M. N. Harakeh and A. van der Woude, *Giant Resonances, Fundamental High-Frequency Modes of Nuclear Excitation* (Clarendon, Oxford, 2001).
[4] Y. Alhassid, J. Zingman, and S. Levit, Nucl. Phys. A **469**, 205 (1987).
[5] M. Kicińska-Habior *et al.*, Phys. Rev. C **36**, 612 (1987).
[6] A. Bracco *et al.*, Phys. Rev. Lett. **62**, 2080 (1989).
[7] P. F. Bortignon, A. Bracco, D. Brink, and R. A. Broglia, Phys. Rev. Lett. **67**, 3360 (1991).
[8] W. E. Ormand, F. Camera, A. Bracco, A. Maj, P. F. Bortignon, B. Million, and R. A. Broglia, Phys. Rev. Lett. **69**, 2905 (1992).
[9] D. Kusnezov, Y. Alhassid, and K. A. Snover, Phys. Rev. Lett. **81**, 542 (1998).
[10] M. P. Kelly, K. A. Snover, J. P. S. van Schagen, M. Kicińska-Habior, and Z. Trznadel, Phys. Rev. Lett. **82**, 3404 (1999).
[11] A. Maj *et al.*, Nucl. Phys. A **731**, 319 (2004).
[12] S. Bhattacharya *et al.*, Phys. Rev. C **77**, 024318 (2008).
[13] D. R. Chakrabarty, V. M. Datar, S. Kumar, E. T. Mirgule, A. Mitra, V. Nanal, R. G. Pillay, and P. C. Rout, J. Phys. G: Nucl. Part. Phys. **37**, 055105 (2010).
[14] D. Pandit *et al.*, Phys. Rev. C **81**, 061302(R) (2010).
[15] S. Mukhopadhayay *et al.*, Phys. Lett. B **709**, 9 (2012).
[16] D. Pandit, S. Mukhopadhyay, S. Bhattacharya, S. Pal, A. De, and S. R. Banerjee, Phys. Lett. B **690**, 473 (2010).
[17] D. Pandit, S. Mukhopadhyay, S. Pal, A. De, and S. R. Banerjee, Phys. Lett. B **713**, 434 (2012).
[18] D. Pandit, B. Dey, D. Mondal, S. Mukhopadhyay, S. Pal, S. Bhattacharya, A. De, and S. R. Banerjee, Phys. Rev. C **87**, 044325 (2013).
[19] Balaram Dey *et al.*, Phys. Lett. B **731**, 92 (2014).
[20] P. Heckman *et al.*, Phys. Lett. B **555**, 43 (2003).
[21] Nguyen Dinh Dang, Phys. Rev. C **84**, 034309 (2011).
[22] D. Pandit, S. Bhattacharya, B. Dey, D. Mondal, S. Mukhopadhyay, S. Pal, A. De, and S. R. Banerjee, Phys. Rev. C **88**, 054327 (2013).

[23] L. Trippa, G. Colo, and E. Vigezzi, Phys. Rev. C **77**, 061304(R) (2008).
[24] H. A. Bethe, Phys. Rev. **50**, 332 (1936).
[25] F. Pühlhofer, Nucl. Phys. A **280**, 267 (1977).
[26] W. Dilg, W. Schantl, H. Vonach, and M. Uhl, Nucl. Phys. A **217**, 269 (1973).
[27] A. V. Ignatyuk, G. N. Smirenkin, and A. S. Tishin, Yad. Fiz. **21**, 485 (1975) [Sov. J. Nucl. Phys. **21**, 255 (1975)].
[28] S. K. Kataria, V. S. Ramamurthy, and S. S. Kapoor, Phys. Rev. C **18**, 549 (1978).
[29] C. Budtz-Jorgensen and H. H. Knitter, Nucl. Phys. A **490**, 307 (1988).
[30] I. Dioszegi, I. Mazumdar, N. P. Shaw, and P. Paul, Phys. Rev. C **63**, 047601 (2001).
[31] S. Mukhopadhayay *et al.*, Nucl. Instrum. Methods A **582**, 603 (2007).
[32] D. Pandit, S. Mukhopadhyay, S. Bhattacharya, S. Pal, A. De, and S. R. Banerjee, Nucl. Instrum. Methods A **624**, 148 (2010).
[33] K. Banerjee *et al.*, Nucl. Instrum. Methods A **608**, 440 (2009).
[34] H. Nifennecker and J. A. Pinston, Annu. Rev. Nucl. Part. Sci. **40**, 113 (1990).
[35] J. R. Huizenga, H. K. Vonach, A. A. Katsanos, A. J. Gorski, and C. J. Stephen, Phys. Rev. **182**, 1149 (1969).
[36] W. Reisdorf, Z. Phys. A **300**, 227 (1981).
[37] H. Nakada and Y. Alhassid, Phys. Rev. Lett. **79**, 2939 (1997).
[38] T. von Egidy and D. Bucurescu, Phys. Rev. C **72**, 044311 (2005).